LRP 559/96 October 1996

Papers presented at the

16th IAEA Fusion Energy Conference

Montréal, Canada, 7-11 October, 1996

LIST OF CONTENTS

Page

- INFLUENCE OF THE SHAPE ON TCV PLASMA PROPERTIES
  J.M. Moret, H. Weisen, S. Franke, M. Anton, R. Behn, B.P. Duval, F. Hofmann, B. Joye, Y. Martin, Ch. Nieswand, Z.A. Pietrzyk, W. van Toledo 1

- RESISTIVE WALL STABILIZATION BY TOROIDAL ROTATION: EFFECTS OF PARTIAL WALL CONFIGURATIONS AND ASPECT RATIO
  D.J. Ward 7

INTERNATIONAL ATOMIC ENERGY AGENCY

SIXTEENTH IAEA FUSION ENERGY CONFERENCE

Montréal, Canada, 7–11 October 1996

IAEA-CN-64/AP1-7

INFLUENCE OF THE SHAPE ON TCV PLASMA PROPERTIES

J.-M. MORET, H. WEISEN, S. FRANKE, M. ANTON, R. BEHN, B.P. DUVAL, F. HOFMANN, B. JOYE, Y. MARTIN, C. NIESWAND, Z.A. PIETRZYK, W. VAN TOLEDO

Centre de Recherches en Physique des Plasmas
Association EURATOM - Confédération Suisse
École Polytechnique Fédérale de Lausanne, CH-1015 Lausanne, Switzerland

INFLUENCE OF THE SHAPE ON TCV PLASMA PROPERTIES

J.-M. MORET, H. WEISEN, S. FRANKE, M. ANTON, R. BEHN, B.P. DUVAL, F. HOFMANN, B. JOYE, Y. MARTIN, C. NIESWAND, Z.A. PIETRZYK, W. VAN TOLEDO

Centre de Recherches en Physique des Plasmas
Association EURATOM - Confédération Suisse
École Polytechnique Fédérale de Lausanne, CH-1015 Lausanne, Switzerland

Energy confinement time of ohmic L-mode plasmas was observed to depend strongly on the shape, improving slightly with elongation and degrading strongly at positive triangularity. This dependence can be explained by geometrical effects on temperature gradient combined with power degradation, without invoking a poloidal variation or a shape dependence of the transport coefficients. The variation with the shape of the sawtooth and Mirnov activity of these plasmas may be the consequence rather than the cause of the change in the confinement.

1. INTRODUCTION

TCV has the unique capability of creating a wide variety of plasma shapes, controlled by 16 independent coils. This opens a new domain in Tokamak operation which has been explored to investigate the influence of the shape on plasma properties. In limited ohmic L-mode stationary discharges ($R = 0.88$ m, $a = 0.25$ m, $B_T = 1.4$ T), the following parameters have systematically been scanned: elongation: $\kappa = 1.1 \rightarrow 1.9$; edge safety factor: $q_a = 2 \rightarrow 6$; triangularity: $\delta = -0.45 \rightarrow 0.75$; line average density: $n_e = 2 .5 \rightarrow 8.5 \times 10^{19}$ m^{-3}. The confinement properties of these plasmas are quantified by the electron energy confinement time, $\tau_{Ee} = W_e/P_{oh}$, where P_{oh} is the ohmic input power. The total electron energy, W_e, is obtained by volume integration of Thomson scattering measurements at 10 spatial positions. For a given plasma shape, τ_{Ee} exhibits the usual increase with q_a and the usual linear dependence on the density. In all conditions a strong dependence of τ_{Ee} on the plasma shape was found: a slight improvement with elongation and a marked degradation with positive triangularity, both at fixed value of q_a (fig. 1a, -

symbols). The degradation factor over the scanned triangularity range is typically 2 and reaches 3 at the highest density [1]. Variation in P_{rad}/P_{oh} are small and cannot account for the change in confinement [2].

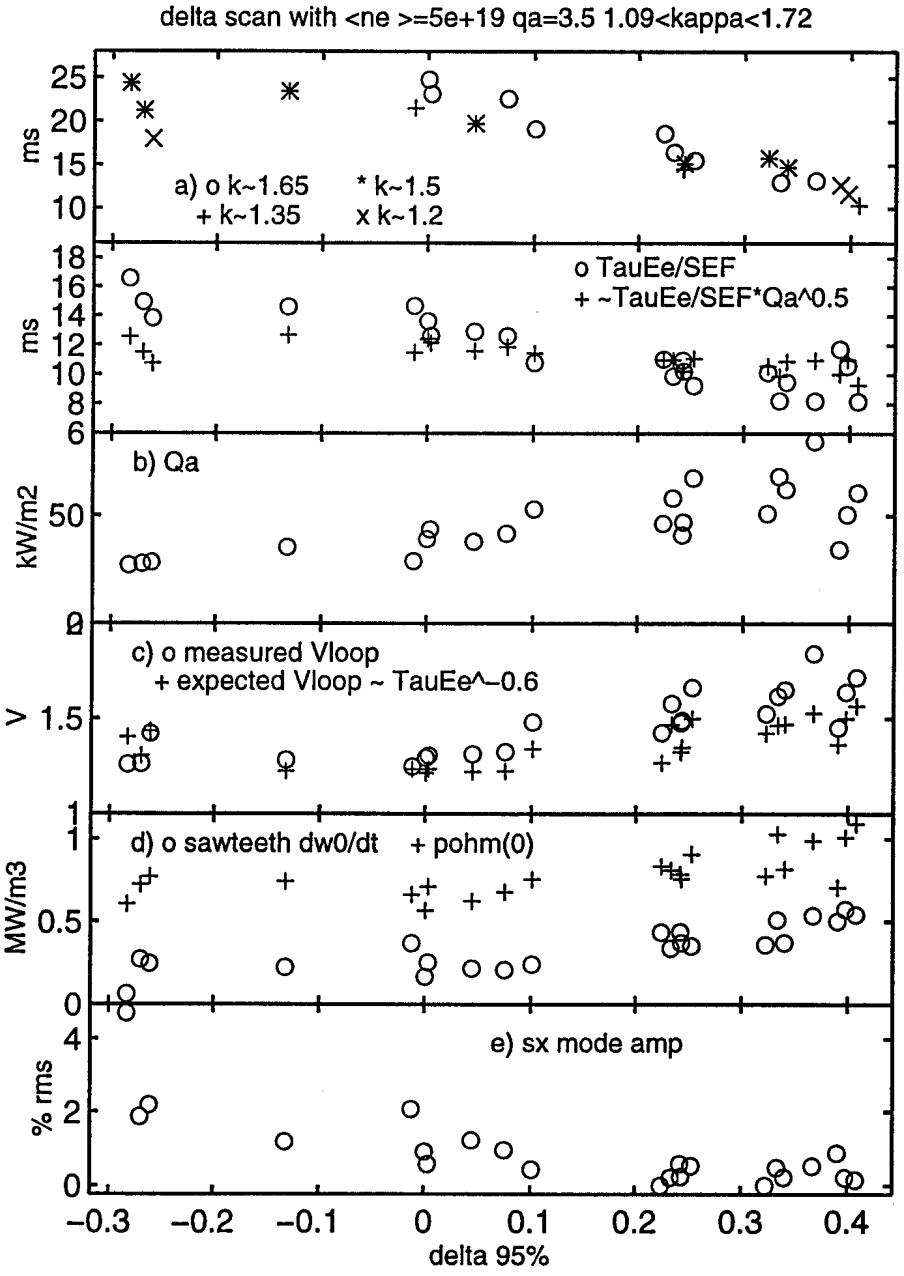

Fig. 1. Shape dependence of relevant parameters.

2. TRANSPORT

A direct consequence of the shaping is a modification of the flux surface separation and incidently of the gradients. This will influence the conducted energy fluxes $q = -n\chi \nabla T$. The density n, the thermal diffusivity χ and the temperature T of both the ions and the electrons are assumed constant on a poloidal flux (ψ) surface. Because the normalised flux coordinate depends on the current distribution, the profiles were mapped on to the equatorial plane. The energy flux becomes $-n\chi\ (dT/dr)\ (dr/d\psi)\ \nabla\psi$ where r is the distance from the magnetic axis measured on the outer equatorial plane and normalised such that it equals the minor radius on the last closed flux surface (LCFS). The spatial distribution of the geometrical factor $(dr/d\psi)\ \nabla\psi$ is plotted in figure 2 for two shapes. This shows how the compression of flux surfaces toward the outer tip of a positive triangularity shape creates an extended region with increased gradients. At negative triangularity, this region shrinks due to increasing separation of the flux surfaces away from the equatorial plane, so that a large part of the plasma can benefit from favorable shaping.

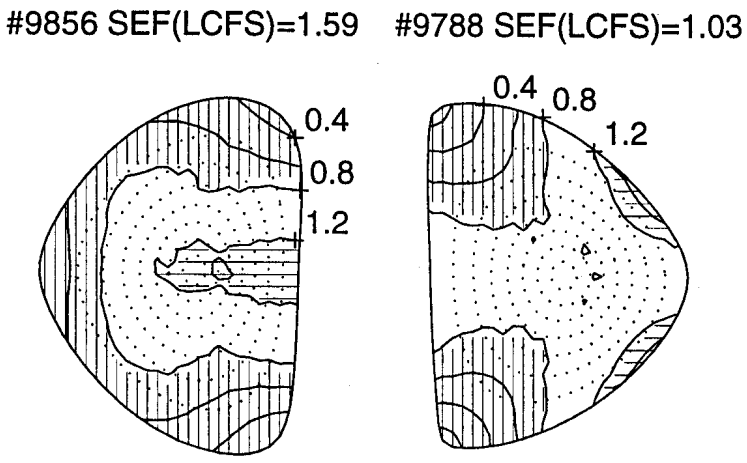

Fig. 2. Distribution of the gradient geometrical factor for a negative (left) and positive (right) triangularity. Vertical and horizontal hatching shows the reduced and increased gradient regions respectively.

To quantify this geometrical effect on the confinement time, one can compare the thermal energy of a shaped plasma with that of a circular plasma with the same thermal conduction and the same power deposition. From $<q> =$

$-n\chi\ (dT/dr)\ (dr/d\psi) \langle\nabla\psi\rangle = P/S$, where P is the power crossing a flux surface and S its area, the temperature profile and the corresponding thermal energy can be derived. It is then convenient to define a Shape Enhancement Factor as the ratio of this energy to that of a similar circular plasma (indexed o):

$$H_s = \frac{\int_0^a \left(\int_r^a \frac{P}{n\chi} \frac{\langle\nabla\psi\rangle^{-1}}{S} \frac{d\psi}{dr} dr' \right) dV}{\int_0^a \left(\int_r^a \frac{P}{n\chi} \frac{1}{S_o} dr' \right) dV_o}$$

where flat density profile was assumed. The weighting function $P/n\chi$ was chosen as $(-dT_o/dr)\ S_o$ where T_o is the average of the normalised temperature profile over all conditions. This function is essentially zero up to mid-radius and constant outside, so that gradient geometrical effects are effective in the outer region. Correcting the electron energy confinement time with the H_s factor cancels all dependence on elongation and largely reduces the triangularity dependence (fig.1a, ×-symbols).

This residual variation can be attributed to power degradation. The heat flux at the LCFS decreases with triangularity (fig.1b). This is due in part to the lower average current density for fixed q_a at low δ and in part to the improved confinement which leads to a reduction of the ohmic power necessary to sustain the chosen plasma current. Assuming Spitzer conductivity $\eta \sim T_e^{1.5}$, an ohmic plasma is expected to respond to a change in confinement mainly by dropping its power requirement $P_{oh} \sim (n_e/\tau_{Ee})^{3/5}$, with only a modest increase in stored energy, $W_e \sim (\tau_{Ee}/n_e)^{2/5}$. A drop in P_{oh} and loop voltage in accordance with this expectation is indeed observed as δ is reduced (fig.1c). In fig.1a (+ symbols) a degradation with an exponent of 1/2 was assumed in addition to the geometrical correction. Note that the pertinent parameter for the degradation reconciling all shapes is the power flux $Q_a = P_{oh}/S$, not the total power; in the latter case high elongations would have a lower confinement time.

Another approach is to set up a simplified radial power balance in which: (i) the radiated power, localised near the plasma edge [2], has been neglected; (ii) in the absence of an adequate measurement of the ion temperature profile T_i, ion and electron channel losses were not separated.

Combining the power balance of both species leads to the definition of an effective thermal diffusivity χ_{eff} such that $q_{oh} = -n_e\chi_{eff} <\nabla T_e>$ and $\chi_{eff} = \chi_e + \chi_i (\nabla T_i/\nabla T_e)$, where q_{oh} is the input energy flux. In figure 3 the usual plot of the power flux versus the temperature gradient is drawn for the gradient region. Given the rough assumptions made and the poor accuracy of a local power balance, no significant influence of the shape on the effective thermal diffusivity can be detected. A heat flux degradation effect or alternatively a temperature gradient dependence of the thermal conductibility however appears clearly.

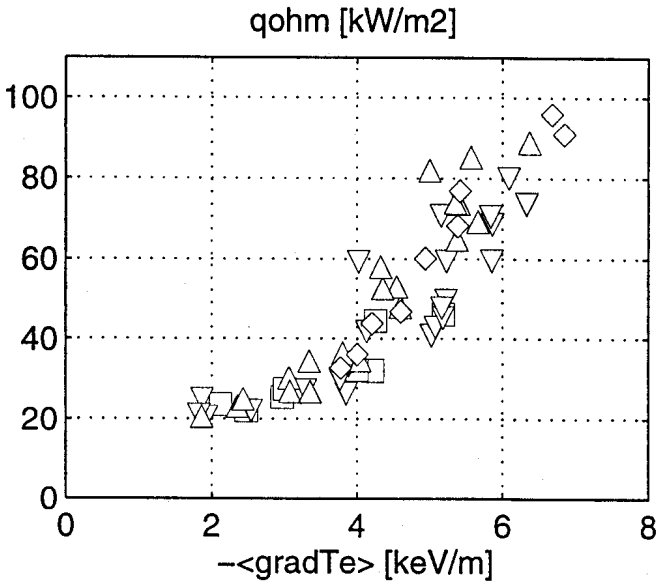

Fig. 3. Power flux versus electron temperature gradient for all shapes and all currents at $n_e = 4.0 \rightarrow 5.5 \times 10^{19}$ m^{-3}. *Symbols represent the trian-gularity:* □ [-0.45,-0.15], ▽ [-0.15,0.15], △ [0.15,0.45], ◇ [0.45,0.75]

3. EFFECT OF SHAPE ON MHD BEHAVIOUR

Sawtooth amplitudes are strongly dependent on triangularity (fig.1d), being largest at positive triangularity and sometimes vanishing at negative triangularity. The sawtooth ramp power density estimated from an X-ray measurement is smaller than the central ohmic power density by typically 0.5 MW/m^3. This is also the minimum ohmic power density necessary to sustain sawteeth in this set of experiments. This power density is believed to correspond to power lost from within the inversion radius by conduction and radiation. MHD mode activity is present as brief bursts at the time of the

sawtooth collapses for $\delta > 0$. As δ is reduced the duration of the bursts of modes increases until they merge into continuous mode activity for $\delta < 0$, often resulting in locked modes and disruptions (fig.1e). The reduction of sawtooth amplitudes at low δ is not due to a significant change of the inversion radius. It can be explained in part by a reduction of the central heating by about 0.2 MW/m^3 due to the improved confinement at low δ. The additional power drained by strong MHD modes at $\delta < 0$ can lead to total suppression of sawteeth as seen for $\delta = -0.28$ in fig.1. The dependence of mode activity on δ may be due to strong reduction of the heat flux at the LCFS at low δ, leading to reduced edge temperatures which may destabilise resisitive modes. An intrinsic dependence of mode stability on plasma shape may also play a role.

4. CONCLUSION

In summary, the large variation in global energy confinement time within the domain of explored shapes can be explained by direct geometrical effects combined with heat flux degradation, without the need to invoke a poloidal variation or a shape dependence of the transport coefficients. Changes in MHD activity may largely result from confinement changes rather that being their cause. These conclusions may not apply to other operational regimes, such as auxiliary heated plasmas or near stability limits, as suggested by DIII–D results [3]. This work however indicates that a global confinement optimisation can be achieved by tuning the plasma shape. Negative triangularity, which may exhibit poor MHD or vertical stability [4], is not the only option. More general shapes can be envisaged which could result from a compromise between the benefits of the geometry and other constraints.

We thank the entire TCV team for their technical effort. This work was partly supported by the Fonds National Suisse de la Recherche Scientifique.

REFERENCES

[1] J.-M. Moret et al., *How the Shape influences the Plasma Properties of TCV, 23rd EPS Conf. on Cont. Fusion and Plasma Phys., Kiev, 1996.*

[2] H. Weisen et al., *Measurement and Modelling of Light Impurity Behaviour in TCV, 23rd EPS Conf. on Cont. Fusion and Plasma Phys., Kiev, 1996.*

[3] A.W. Hyatt, E.A. Lazarus, T.H. Osborne, *21st EPS Conf. on Cont. Fusion and Plasma Phys., Montpellier, 1994,* p. 14, vol. 18B part I.

[4] M.J. Dutch et al., *22nd EPS Conf. on Cont. Fusion and Plasma Phys., Bournemouth, 1995,* p. 77, vol. 19C part IV

INTERNATIONAL ATOMIC ENERGY AGENCY

SIXTEENTH IAEA FUSION ENERGY CONFERENCE

Montréal, Canada, 7–11 October 1996

IAEA-CN-64/ DP-2

Resistive Wall Stabilization by Toroidal Rotation: Effects of Partial Wall Configurations and Aspect Ratio

D. J. Ward

Centre de Recherches en Physique des Plasmas,
Association Euratom - Confédération Suisse,
Ecole Polytechnique Fédérale de Lausanne,
CH-1015 Lausanne, Switzerland

F1-CN-64/DP-2

Resistive Wall Stabilization by Toroidal Rotation: Effects of Partial Wall Configurations and Aspect Ratio

Abstract

Toroidal rotation of the plasma coupled with resistive walls can fully stabilize pressure-driven kink modes and allow the beta value to be extended beyond the Troyon limit. It is well understood that for a rotating resistive wall mode (RWM), the mode is more stable when the wall is moved farther away, as long as the wall is close enough to stabilize the ideal plasma mode. By introducing gaps in the resistive wall — an effect similar to moving the wall away — the RWM can be stabilized at a lower rotation frequency. This effect is greatly enhanced by gaps near the outboard midplane, where the pressure-driven kink couples most strongly to the wall. This improvement in stabilization comes at the cost of requiring a closer wall to stabilize the ideal plasma mode. But this trade-off can be quite desirable: it will be shown that an advanced tokamak equilibrium can be stabilized by a pair of close-fitting plates at a rotation frequency reduced by a factor of 3.6 compared to a fully surrounding wall while maintaining ideal stability.

Increasing the number of rational surfaces residing in the plasma is also seen to lower the necessary rotation frequency needed to stabilize the RWM. By lowering the aspect ratio, and thereby increasing the toroidal coupling and the number of rational surfaces inside the plasma, the necessary rotation frequency can be greatly reduced. An optimized low-aspect-ratio equilibrium with 55% beta can be fully stabilized against the n=1 pressure-driven kink with ω_T/ω_A =0.005.

I. Introduction

Numerical calculations [1,2] have shown that it is possible to stabilize pressure-driven kink modes, where the value for β (the ratio of the plasma particle pressure to the magnetic field pressure) is above the Troyon limit, in a tokamak plasma surrounded by a resistive wall given sufficient toroidal rotation. Experimental results [3,4] have confirmed this stabilizing effect.

There are, in fact, two modes which must be stabilized simultaneously [1,2]: (1) the ideal "plasma mode", and (2) the "resistive wall mode" (RWM). The plasma mode is stable when the wall separation is less than the marginal position for stability with an ideally conducting wall. The resistive wall mode is stable for a given (sufficient) rotation when the wall separation is larger than some marginal value. This results in a region of stability, in terms of wall position, for a given rotation speed. Increasing the rotation speed moves the marginal position for stability of the resistive wall mode closer to the plasma, thus widening the stability region. Conversely, by moving the resistive wall farther from the plasma (but remaining always within the marginal ideal wall threshold), the resistive wall mode can be stabilized at a lower rotation speed.

Introducing gaps in the wall has much the same effect as moving the wall farther away, in that it is easier to stabilize the resistive wall mode (i.e., the resistive wall mode can be stabilized at a lower rotation speed). For pressure-driven, external kink modes, the instability couples most strongly to the wall at the outboard midplane. Therefore, toroidally continuous gaps near the outboard midplane can have a very strong effect. This effect moves the region of stability, in terms of wall position, closer to the plasma and reduces it in extent, but allows stabilization to be reached at a lower rotation speed. This effectively makes wall stabilization more accessible.

Toroidal coupling between different poloidal harmonics and between the Alfvén and sound waves complicates the effect of rotation on pressure-driven modes. Rotation modifies the eigenfunction at resonances near the rational surfaces, and calculations indicate [2,4] that additional rational surfaces, particularly those in regions of relatively high pressure, make the stabilization more effective. The effect of lower aspect ratio, which increases toroidal coupling and the number of rational surfaces residing in the plasma, on resistive wall stabilization will be examined in Section III.

II. Partial Wall Configurations

Because of the importance of wall stabilization for advanced tokamak equilibria [5] (that is, equilibria with reverse-shear, high-β, high bootstrap fraction) we will focus on such equilibria in this section. The equilibrium considered here is a reverse-shear equilibrium used in calculations presented in Ref. [2]. This particular equilibrium is identical to that in Fig. 9 of Ref. [2] at $\beta^* = 5.2\%$ (β^* is the rms value of β, i.e., $\beta^* \equiv 2\mu_0\langle p^2\rangle^{1/2}/\langle B^2\rangle$). This equilibrium is very similar to the equilibria described in Ref. [5]. It has $q_0 = 2.5$, $q_{min} \approx 2.2$, $q_s = 4.1$, high β^*, and a bootstrap fraction of nearly unity with the bootstrap current well aligned with the total plasma current. It is stable everywhere to ballooning modes and has good stability properties with respect to various microinstabilities [5], but is unstable to the low-n pressure-driven, external kink. In the absence of a conducting wall, the limit in β^* is 2.49%.

Figure 1: Stabilization of high-pressure kink with outboard gaps

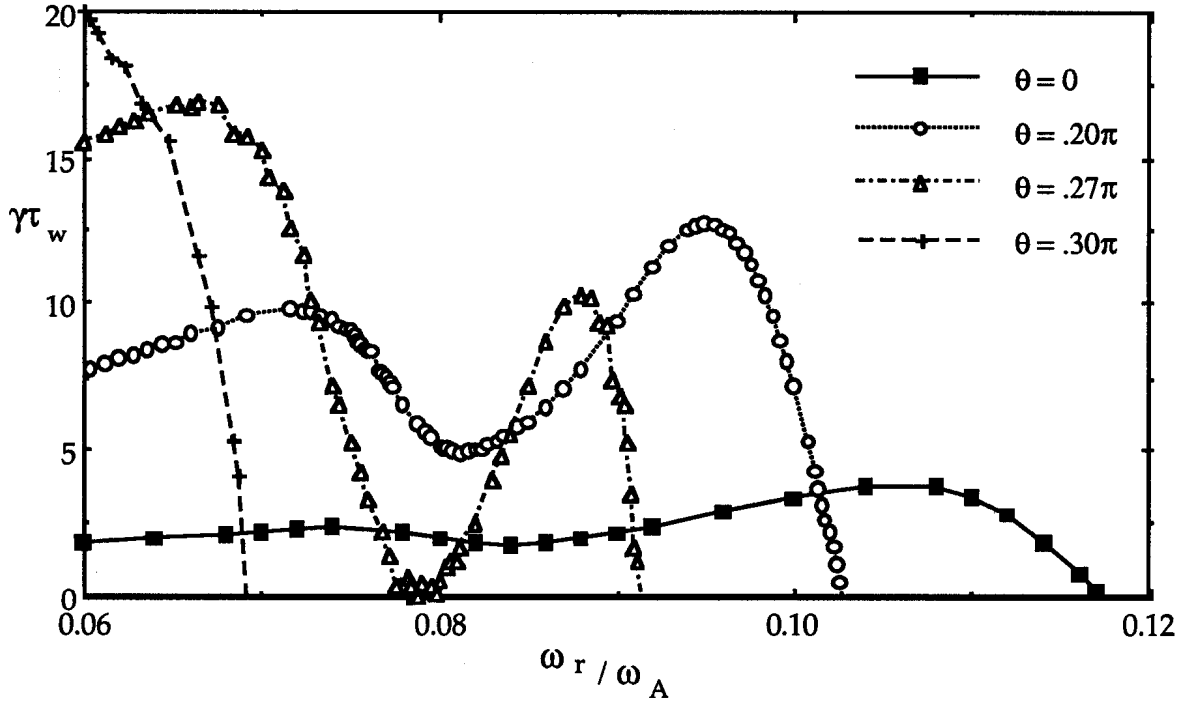

Figure 1 shows the results with a wall separation of $d/a = 1.04$ and with gaps in the wall centered at the *outboard* midplane with half-widths of $\theta_g = 0.2\pi$, $\theta_g = 0.27\pi$, and a slightly larger gap of $\theta_g = 0.3\pi$, as well as for $\theta_g = 0$ (full wall). For $\theta_g = 0.2\pi$, the threshold rotation frequency above which the resistive wall mode is stabilized is $\omega_r/\omega_A \approx 0.103$ — a reduction of 13% from the case with a full wall. For a somewhat larger outboard gap of half-width $\theta_g = 0.27\pi$, the threshold rotation frequency is $\omega_r/\omega_A \approx 0.092$ — a 22% reduction from the case with a full wall.

Figure 1 shows that the threshold stability value of ω_r for the case with an outboard gap of $\theta_g = 0.3\pi$ is $\omega_r/\omega_A \approx 0.069$. This is a reduction of 41% of the necessary rotation frequency to stabilize compared to the case with a full wall. The necessary wall separation needed to stabilize the ideal plasma mode is $d/a = 1.06$ for the case with an outboard gap of $\theta_g = 0.3\pi$, compared to $d/a = 1.36$ for the full wall. This results in the need to have the wall somewhat

closer in order to stabilize the ideal plasma mode when there is such a gap, but there is a significant reduction in the necessary rotation to stabilize the resistive wall mode.

II.A. Wall Stabilization with Discrete Conducting Plates

In the Tokamak Physics Experiment (TPX) design [6] passive stabilization against the axisymmetric, vertical instability and against the ideal external kink is provided by conducting plates on the inboard and outboard sides. In fact, the passive structure is not quite axisymmetric and actually takes the form of a three-dimensional "cage". But it can be approximated as two pairs of axisymmetric plates. A resistive wall on the inboard side has very little effect on the pressure-driven kink mode in high-β equilibria; therefore the inboard plates will be ignored in the following calculations. The calculations use a pair of conformal wall sections on the outboard side with the same poloidal angular extent as the outboard TPX plates (from $|\theta| = 0.18\pi$ to $|\theta| = 0.48\pi$).

The results are shown in Fig. 2. The growth rates are normalized to the same wall time (calculated for a complete resistive wall) as in Fig. 1. Here we see that the growth rates are considerably higher than for the cases in Fig. 1, particularly in the peak just short of the critical rotation frequency for stabilization. But we see that stabilization occurs at a much lower rotation frequency. In fact, the necessary critical frequency for stabilization is reduced by a factor of aprroximately 3.6 compared to the case with a complete wall with the same plasma–wall separation (with a full wall at $d/a = 1.04$ there is stabilization at $\omega_T/\omega_A \approx 0.12$).

Therefore we see that a large outboard gap, or even limiting the nearby conducting structure to a pair of discrete plates, can have a beneficial effect on the stabilization of the resistive wall mode by lowering the necessary rotation speed by a significant factor. There is, of course, a trade-off in that in order to also stabilize the ideal plasma mode (and both modes *must* be stabilized at the same time), the maximum plasma wall separation is reduced. However, it is well understood that any configuration must be stable with an *ideal* wall. These results show that for a configuration with close-fitting plates, or a wall with a large outboard gap, the necessary rotation speed for stabilization of the resistive wall mode is greatly reduced compared to that which would be necessary with a continuous, completely surrounding resistive wall.

Figure 2: TPX-like equilibrium with close-fitting, discrete conducting plates

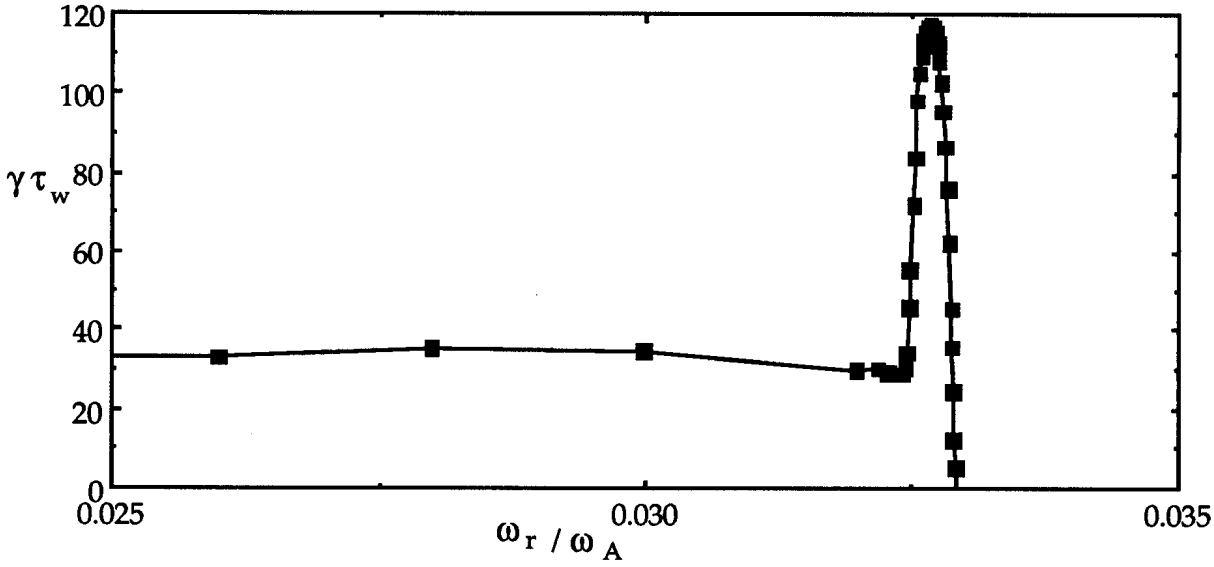

III. Resistive Wall Stabilization of Low-Aspect-Ratio Tokamaks

The stabilization of resistive wall modes by toroidal rotation requires resonant surfaces inside the plasma [1,2], and toroidicity plays an important role in this stabilizing effect. Previous results [2] have indicated that the presence of a larger number of rational surfaces in

the plasma enhances this stabilizing effect. It seems likely, therefore, that resistive wall stabilization may be more effective for low-aspect-ratio equilibria, in which toroidal effects are enhanced, and in which a large number of rational surfaces naturally reside in the plasma.

Table I shows the results of resistive wall calculations for various aspect ratios. The table lists characteristics of the equilibria, such as inverse aspect ratio ε, values of β and β^*, the normalized values of beta (g and g^*), the ratio of the normalized beta for the equilibrium to that for the corresponding equilibrium which is marginally stable to the free-boundary kink mode ($g/g_{\rm lim}$), q at the surface, the growth rate (without rotation) normalized to the wall time (for a wall at $d/a = 1.05$), the ideal wall position for marginal stability, and finally the value of rotation that stabilizes the resistive wall mode (for a wall at $d/a = 1.05$). A scan was made of the aspect ratios $\varepsilon = 0.3$, 0.6, and 0.7; the definition for the profiles was kept the same, and the magnitude of the pressure was varied to make equilibria that are unstable to the pressure-driven kink. The characteristic values for the marginally stable ($g/g_{\rm lim} = 1.00$) equilibria are also shown for those three aspect ratios.

We see that the magnitude of $\gamma\tau_W$ (without rotation) and the value of d/a(ideal) are both good measures of the strength of the instability, and are inversely correlated. As the instability becomes stronger (higher growth rate) it takes a larger rotation speed to stabilize it. Therefore it is quite striking that at the higher values of ε (0.6 and 0.7) the equilibria listed here are very unstable (by a factor of over thirty, in one case, over the $\varepsilon = 0.3$ unstable equilibrium), and yet the necessary rotation speed is quite comparable to that required to stabilize the $\varepsilon = 0.3$ case. A useful measure of how difficult it is to stabilize the RWM is the ratio of the rotation speed needed to stabilize the RWM divided by the passive growth rate with no stabilization. Note that the equilibria in the aspect-ratio scan (with the exception of the last equilibrium) are not optimized in any way, and consequently the equilbria at low aspect ratio are considerably more unstable than for the higher aspect ratio cases.

Table I: Aspect-ratio scan

ε=1/A	β	β^*	g	g^*	$g/g_{\rm lim}$	q_s	$\gamma\tau_W$	d/a(ideal)	ω_s/ω_A
0.3	5.153	5.848	2.67	3.03	1.00	4.12	0.00	∞	0.00
0.3	6.026	6.841	3.165	3.593	1.185	4.279	1.33	1.44	0.0236
0.6	14.05	15.98	4.17	4.74	1.00	9.05	0.00	∞	0.00
0.6	15.28	17.35	4.638	5.267	1.112	9.493	2.78	1.275	0.0182
0.6	17.26	19.61	5.49	6.237	1.316	10.41	12.44	1.112	0.035
0.7	18.13	20.60	5.285	6.003	1.00	15.99	0.00	∞	0.00
0.7	18.72	21.27	5.557	6.314	1.052	16.67	42.75	1.07	0.0312
0.7	19.78	22.48	6.083	6.915	1.151	18.18	24.17	1.092	0.0144
0.714	40.59	43.59	6.313	6.780	N/A	14.83	2.735	1.26	0.0047

The final equilibrium listed in Table I ($\varepsilon = 0.714$) is a highly optimized (to give high beta, ballooning stability, and near unity bootstrap fraction) low-aspect-ratio equilibrium developed by R. L. Miller et al. [7]. In this case very high values of beta are achieved ($\beta_X = 55\%$, where $\beta_X \equiv 2\mu_0\langle p\rangle/B_0^2$ — here, B_0 is the magnetic field at the axis, following the convention commonly used for defining beta at low aspect ratio), and yet the passive growth rate is only $\gamma\tau_W = 2.735$, and the equilibrium is completely stabilized (with a wall separation of $d/a = 1.05$) at a normalized rotation speed of less than 0.005. Figure 3 shows the normalized growth rate for this case with respect to normalized rotation speed. Therefore, we see that this highly optimized, high-β equilibrium is stabilized at quite modest values of rotation speed.

Figure 3: Optimized low-aspect-ratio equilibrium

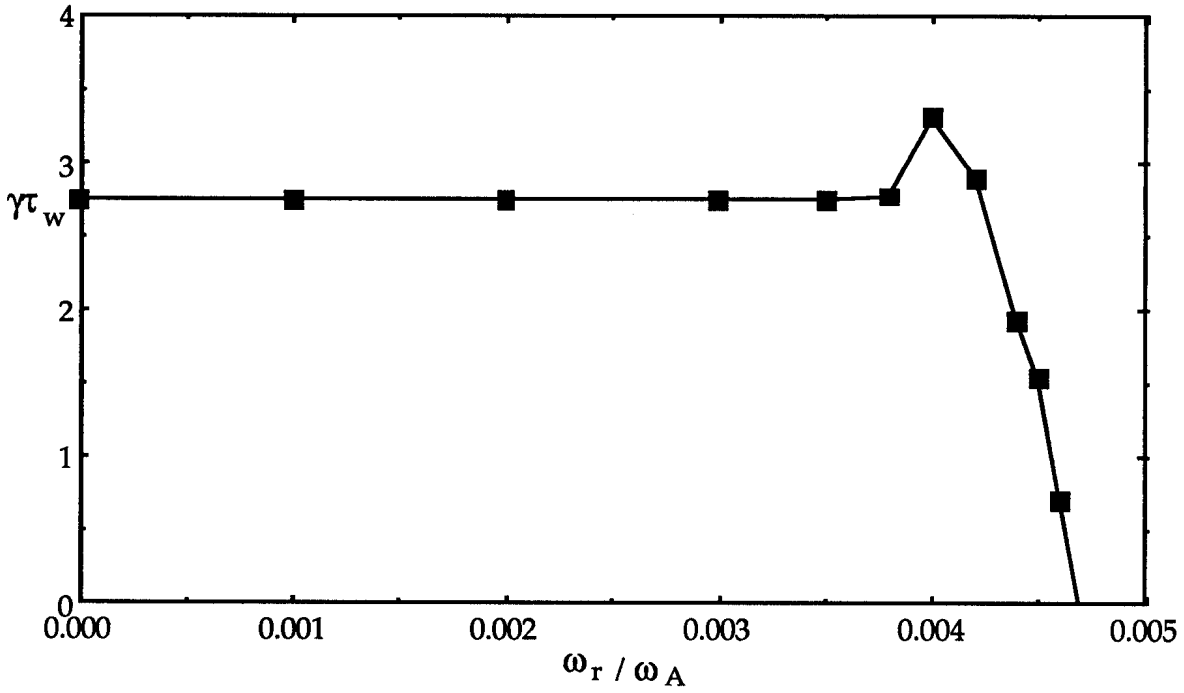

Figure 4: Ratio of stabilizing ω to passive growth rate vs. # of rational surfaces

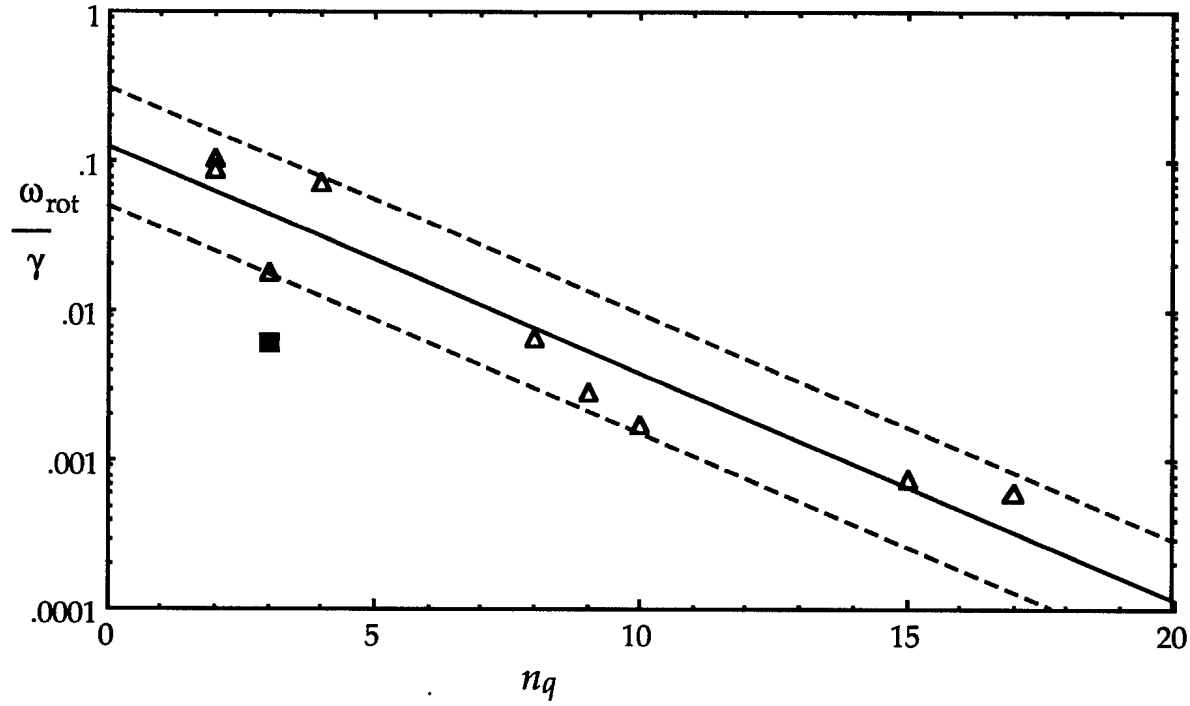

Figure 4 shows the ratio of the rotation speed necessary to stabilize the RWM (normalized to the Alfvén time) divided by the growth rate (normalized to the wall time) at zero rotation. The denominator measures the strength of the instability, and the numerator measures how much rotation is needed for stabilization. This ratio is plotted versus the number of rational surfaces inside the plasma. The points plotted are for 10 different equilibria with varying

profiles, shape, aspect ratio, etc. The solid line is a fit to the results (resulting in an exponential, since this is a log–linear plot), and the dotted lines are parallel to and differ by a magnitude of 2.5 higher or lower than the fit. One can see that all 9 triangular points lie within the factor of 2.5 from the line. Only the solid square falls outside the region, and this is a somewhat special case: the PBX-M experimental equilibrium analyzed in Ref. [4]. It is the only equilibrium tested here which has a q=1 surface, and it was seen that the eigenfunction was strongly modified at the q=1 surface, which lies well within the high-pressure region of the equilibrium and was noticeably more affected by the rotation and damping than the other surfaces.

We learn from Fig. 4 that there is a strong reduction in the necessary rotation speed necessary to stabilize a RWM with a given passive growth rate as the number of rational surfaces inside the plasma is increased. Therefore, the stabilizing effect is greatly enhanced by increasing the number of q surfaces inside the plasma, and thus low-aspect-ratio equilibria benefit, since by their nature they have high q at the edge and many rational surfaces. This agrees qualitatively with the work of Bondeson and Chu [8], which shows that there is a toroidal inertia enhancement with increasing edge-q so that the mode structure is drastically changed (thus enhancing the stabilizing effect of rotation) when the rotation exceeds a crititcal value that is approximately $\omega_r > \omega_A/4q^2$.

The result of enhanced stabilization with increasing number of rational surfaces is general, and if the equilibrium is also optimized to minimize the instability (i.e., the growth rate in the absence of rotation) while maximizing beta and other favorable quantities, such as in the last entry of Table I, the optimized low-aspect-ratio equilibrium of Ref. [7] (the point in Fig. 4 at n_q=10), it can be fully stabilized at a reasonably low rotation speed, as seen in Fig. 3.

Summary

Results have been presented which demonstrate that gaps in the resistive wall, particularly at the outboard midplane, can significantly reduce the necessary rotation speed to stabilize the RWM at the cost of requiring a somewhat closer wall for ideal stability. In particular, it was shown that with a pair of close-fitting conducting plates (which leave a large gap at the outboard midplane) a high-β equilibrium at conventional aspect ratio can be stabilized at a rotation speed reduced by a factor of over 3.5 compared to a fully surrounding, continuous and complete wall at the same separation, while maintaining stability to the ideal plasma mode.

The results also show that low-aspect-ratio equilibria can be stabilized at significantly lower rotation speeds than those for equilibria at conventional aspect ratio. There is a definite reduction in the necessary rotation speed needed to stabilize an instability with a given growth rate as the number of rational surfaces inside the plasma increases. These two effects can perhaps be combined to enhance even further the effect of resistive wall stabilization at low aspect ratio.

Acknowledgments

I would like to thank R. L. Miller and O. Sauter for helpful discussions and for providing the optimized low-aspect-ratio equilibrium used in Section III. This work was supported by the Fonds National Suisse pour la Recherche Scientifique.

References

[1] A. BONDESON and D. J. WARD, Phys. Rev. Lett. **72** (1994) 2709.
[2] D. J. WARD and A. BONDESON, Phys. Plasmas **2** (1995) 1570.
[3] E. J. STRAIT et al., Phys. Rev. Lett. **74** (1995) 2483.
[4] M. OKABAYASHI et al., to appear in Nucl. Fusion **36** (1996).
[5] C. KESSEL, J. MANICKAM, G. REWOLDT, W. M. TANG, Phys. Rev. Lett. **72** (1994) 1212.
[6] R. GOLDSTON et al., Contr. Fusion and Plasma Phys., Proc. 20th Europ. Conf., Lisbon, 1993 (Europ. Phys. Soc., Petit-Lancy, Switzerland, 1993), Vol. 17C, I- 319.
[7] R. L. MILLER, et al., G.A. Report, GA-A22321, July 1996; submitted to Phys. Plasmas.
[8] A. BONDESON and M. S. CHU, Phys. Plasmas **3** (1996) 3013.